CORRELATION BETWEEN THE CHANGES IN STRUCTURE AND ELECTRICAL RESISTIVITY OF AMORPHOUS METALS

Supplement to Sci. Rep. RITU, A, March, 1980

CORRELATION BETWEEN THE CHANGES IN STRUCTURE AND ELECTRICAL RESISTIVITY OF AMORPHOUS METALS

T. Hanamura, M. Doi, M. Matsui* and T. Imura

Department of Metallurgy, *Department of Iron and Steel Engineering, Faculty of Engineering,

Nagoya University, Nagoya 464, Japan

ABSTRACT

Using electron microscopy and electrical resistivity measurements, structural changes in amorphous alloys, which occurred during heating, were studied over a wide temperature range. Ribbons of Fe-B-Si alloy were prepared by quenching liquid alloy on to cold twin rollers rotating at high speed; several different rotation speeds were used. Amorphous ribbons of $Ni_{80}(P_xB_{1-x})_{20}$ alloys, where X= 0.25, 0.5, 0.75, were made also using one roll speed. Among these ribbons, differences were found in electrical resistivity and its annealing behavior, which depended on the quenching conditions and on the ratio of the contents of two component metalloids. In the system $Ni_{80}(P_xB_{1-x})_{20}$, it was found that the electrical resistivity of the $Ni_{80}P_{10}B_{10}$ alloy specimen had the highest value. It was also found that the electrical resistivity was increased by the cyclic deformation of the liquid-quenched Co-B-Si amorphous alloy. Differences in thermal and mechanical stability of these alloys suggest that so-called amorphous alloys do not have one definite atomic arrangement but have a variety of arrangements, depending on the conditions of preparation.

INTRODUCTION

By rapid quenching from the melt (so-called liquid-quenching or splat-cooling), a large number of alloy systems have been solidified without forming crystalline phase.[1-2] Structural studies have been carried out by the authors' group[3-5] by means of high resolution electron microscopy as well as field-ion microscopy and it has been suggested that different structural states may exist in the liquid-quenched amorphous alloys, depending on the quenching conditions. The properties characteristic of those amorphous alloys should have a close relation to their atomic arrangements. Since electrical resistivity is a structure-sensitive property, it seems possible to obtain more information on structure.

In the present experiments, the temperature dependence of electrical resistivity was measured with Fe-based and Co-based amorphous alloy ribbons which were obtained by liquid-quenching at different rotation speeds of twin rollers. In the system $Ni_{80}(P_xB_{1-x})_{20}$, the changes of electrical resistivity were measured with changing X and structural changes were examined in parallel with the resistivity measurements, by transmission electron microscopy. The changes in stress-strain behavior after cyclic tensile deformation and the changes in the electrical resistivity due to deformation were investigated also.

EXPERIMENTAL

Twin rollers of 50 mm Ø, which were made of carbon tool steel, were used for liquid-quenching and the rotation speeds used were in the range of 3600 r.p.m. to 5400 r.p.m. By using the roller-quenching method (twin-roller method), three kinds of ribbon samples of $Fe_{78}B_{12}Si_{10}$ amorphous alloy were obtained at three different rotation speeds of twin rollers, namely, 3600 r.p.m., 4500 r.p.m. and 5400 r.p.m. Ribbon samples of $Co_{75}B_{10}Si_{15}$, $Ni_{80}P_5B_{15}$, $Ni_{80}P_{10}B_{10}$ and $Ni_{80}P_{15}B_5$ alloy were obtained at 4500 r.p.m. Typical value of cross-sectional area of these ribbon samples was 1 mm X 0.020 mm. All the ribbon samples yielded only diffuse halo rings by X-ray or electron diffraction inspection.

The electrical resistivity measurements were made by a four-probe DC method. Four nickel leads of 0.2 mm in diameter were spot-welded to the ribbon samples. The spacing between the two probes for voltage measurement was 5 mm. The electric current was fixed throughout the experiment at a low value, namely, 100.00 mA to suppress the temperature rise of the sample due to current flow. The experimental errors in electrical resistivity measurements arises mainly from estimation of cross-sectional area which depends on the uniformity in thickness and on the surface roughness. The uniformity in thickness as well as in the breadth of each sample was inspected by using an optical microscope. Since the scatter in thickness (including the roughness of the surface) of each sample was less than ± 0.5 μm, the accuracy of the electrical resistivity measurements in the present experiments was better than ± 3 percent. The temperature was measured with a calibrated Pt.Pd.Au-Pd.Au thermocouples in the temperature range of 4.2 K to room temperature and also with a calibrated chromel-alumel thermocouple in the range of room temperature to 1000 K.

The thin foils of ribbon samples of $Ni_{80}P_5B_{15}$, $Ni_{80}P_{10}B_{10}$ and $Ni_{80}P_{15}B_5$ amorphous alloys which were electro-polished for transmission electron microscope observations were sandwiched in copper grids and heated to desired temperatures between room temperature and 1000 K. During heating, they were placed adjacent to the sample for resistivity measurement (within 5 mm) and electron microscopic observation was carried out with these samples in parallel with the resistivity measurements.

The tensile deformation (including that by load-unload stressing cycles), was performed by using an Instron-type testing machine at room temperature. The tensile test piece of 10 mm - 20 mm in gauge length was prepared from amorphous ribbon which had been inspected by using an optical microscope (at the magnification of 400 times or 1000 times) for confirming the uniformity in thickness and breadth. Specially designed grips were used to grasp the test piece and the elongation was measured by using two differential transformers.

THE DIFFERENCES IN ELECTRICAL RESISTIVITY BY PREPARATION

The electrical resistivity of $Fe_{78}B_{12}Si_{10}$ amorphous alloy liquid-quenched at 4500 r.p.m. is illustrated in Fig. 1 as a function of annealing temperature. The temperature was raised from 4.2 K to 1000 K at the

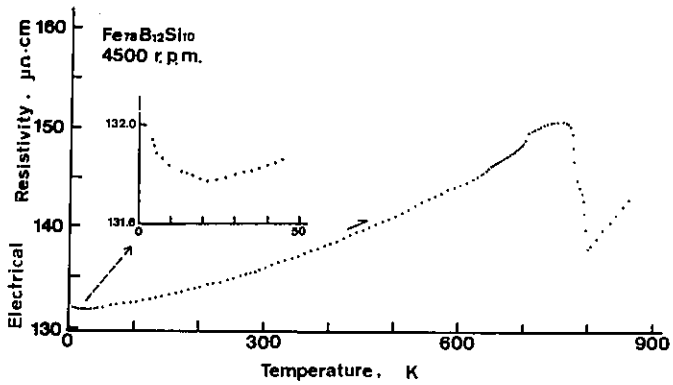

Figure 1. Electrical resistivity of a liquid-quenched Fe-B-Si amorphous alloy expressed as a function of temperature.

rate of about 2 K per minute. The resistivity decreased at first but soon a minimum appeared and then it started to increase gradually. A similar resistivity minimum at cryogenic temperatures has been observed in other amorphous alloys by many investigators, e.g. in Ni-P[6-8], Co-P[8], Fe-Pd-Si[9], Co-Pd-Si[9], Fe-P-C[10], etc. As the temperature was raised from room temperature, the electrical resistivity increased steadily up to about 750 K except a small maximum near 750 K. At about 750 K, the resistivity decreased suddenly, but at about 800 K it started to increase again.

Fig. 2 illustrates the temperature dependence of electrical resistivity obtained from three kinds of liquid-quenched $Fe_{78}B_{12}Si_{10}$ amorphous ribbons which were prepared at different rotation speeds of the rollers, i.e. 3600 r.p.m., 4500 r.p.m., and 5400 r.p.m. The absolute value of the resistivity for each ribbon was different for three rotation speeds. According to the electron-probe microanalysis, the difference in chemical composition between the three amorphous ribbons was negligible. As indicated by open arrows (⇧) in Fig. 2, the temperature at which the decrease in resistivity (due to crystallization) started, was almost the same for each ribbon (this temperature is designated by T_c hereafter). Furthermore, a careful observation shows that the decrease in resistivity of each ribbon occurs in two steps. The second steps are indicated by thin arrows (↑) in the figure.

Detailed examinations made of these curves both before and after crystallization showed that appreciable differences were observed among these ribbons viz.

(1) absolute value of resistivity,
(2) the shape of the curve at the temperature just below T_c, as indicated by bold arrows (⬆),
(3) the temperature at which the temperature coefficient of resistivity changes from negative to positive above T_c, indicated by broken arrows

(?),
(4) the amount of the decrease in resistivity due to crystallization which starts at T_c.

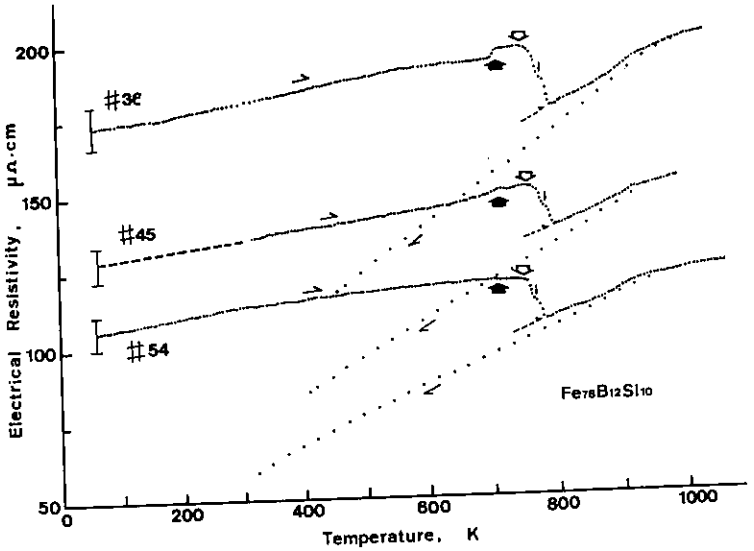

Figure 2. Temperature dependence of electrical resistivity of liquid-quenched Fe-B-Si amorphous ribbons prepared at different rotation speeds of rollers. The notation #36, #45 and #54 indicate rotation speeds of 3600 r.p.m., 4500 r.p.m. and 5400 r.p.m., respectively.

From the differences among these ribbons, it can be easily concluded that liquid-quenching at different rotation speeds of the rollers yielded different structural states in the amorphous alloys.

THE DIFFERENCES IN ELECTRICAL RESISTIVITY BY CHANGING THE RATIO OF TWO COMPONENT METALLOIDS

Fig. 3 illustrates the temperature dependence of electrical resistivity obtained with $Ni_{80}P_5B_{15}$, $Ni_{80}P_{10}B_{10}$ and $Ni_{80}P_{15}B_5$ amorphous alloys. In these three specimens, the value of electrical resistivity from room temperature to about 650 K increased gradually and the absolute value is higher in the specimen of $Ni_{80}P_{10}B_{10}$ than those in the other specimens. The resistivity increases smoothly until crystallization occurs, but then drops rapidly with increasing temperature. The temperatures at which the electrical resistivity decreases are 610 K for $Ni_{80}P_5B_{15}$, 648 K for $Ni_{80}P_{10}B_{10}$ and 624 K for $Ni_{80}P_{15}B_5$. The crystallization temperature of $Ni_{80}P_{10}B_{10}$ alloy is the highest among these three alloys. Heating the specimen further causes the second change. The decrease in resistivity for the change is greatest for the $Ni_{80}P_5B_{15}$ alloy. The further temperature increases in which the second changes occur (i.e. from o to • in Fig. 3) are in the approximate ratio 3:2:1 for X= 0.25, X= 0.5 and X= 0.75, respectively. The larger the ratio of B/P becomes, the larger the temperature interval from o to • becomes. Fig. 4 shows the reversible and irreversible parts of electrical resistivity of $Ni_{80}P_{10}B_{10}$ amorphous alloy as a function of temperature. The specimen heated to 550 K did not show

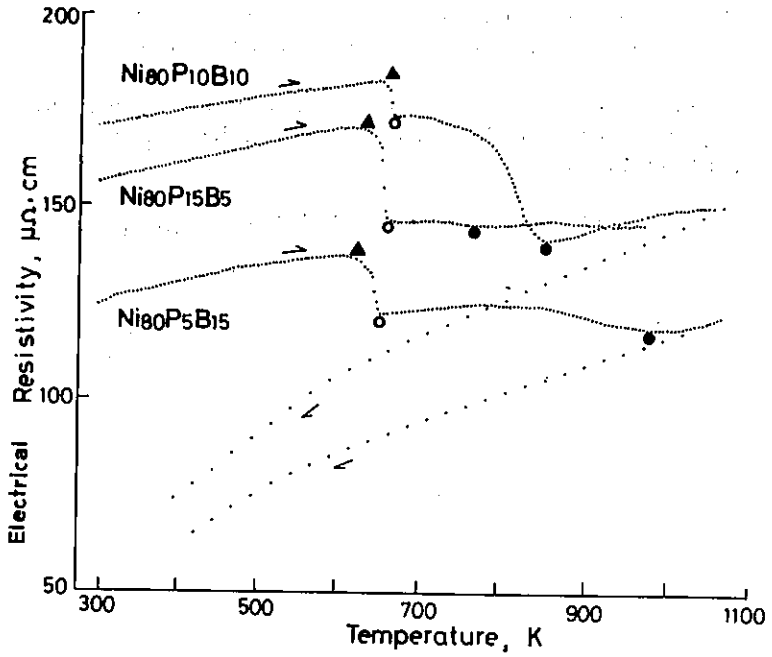

Figure 3. Electrical resistivity vs. temperature curve of $Ni_{80}(P_xB_{1-x})_{20}$ amorphous alloy system.

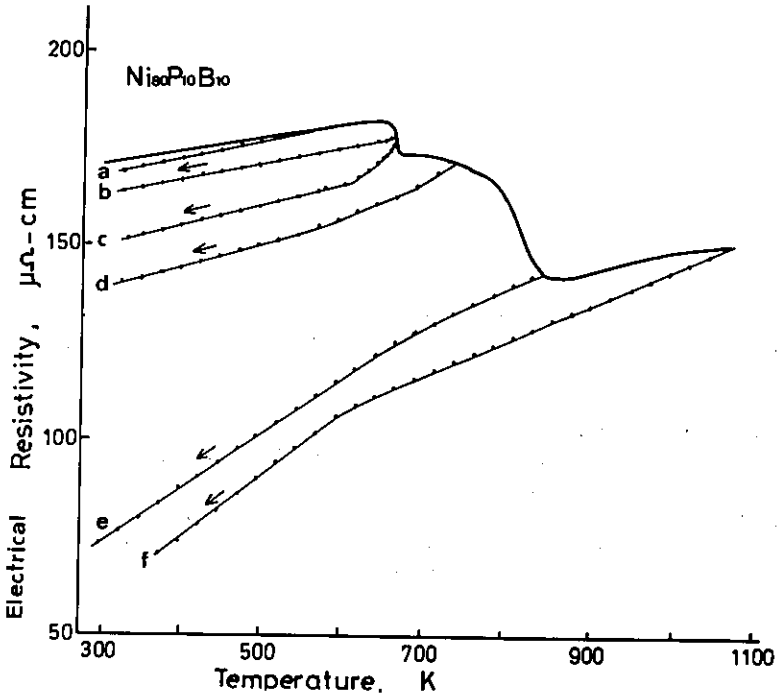

Figure 4. Reversible and irreversible changes of electrical resistivity as a function of temperature.

any irreversible effect, so no structural changes which affected the change in electrical resistivity took place up to this temperature. However, when the specimen was heated to 600 K, the resistivity curve was no longer reversible. This irreversibility is indicative of the occurrence of a kind of structure changes, although conventional electron microscopic observation could not reveal this type of structure changes.

Fig. 5, 6 and 7 are electron micrographs showing structural changes due to annealing in three amorphous alloys, i.e., $Ni_{80}P_{10}B_{10}$, $Ni_{80}P_{15}B_5$, and $Ni_{80}P_5B_{15}$, respectively.

Fig. 5 shows the structural changes in the $Ni_{80}P_{10}B_{10}$ amorphous

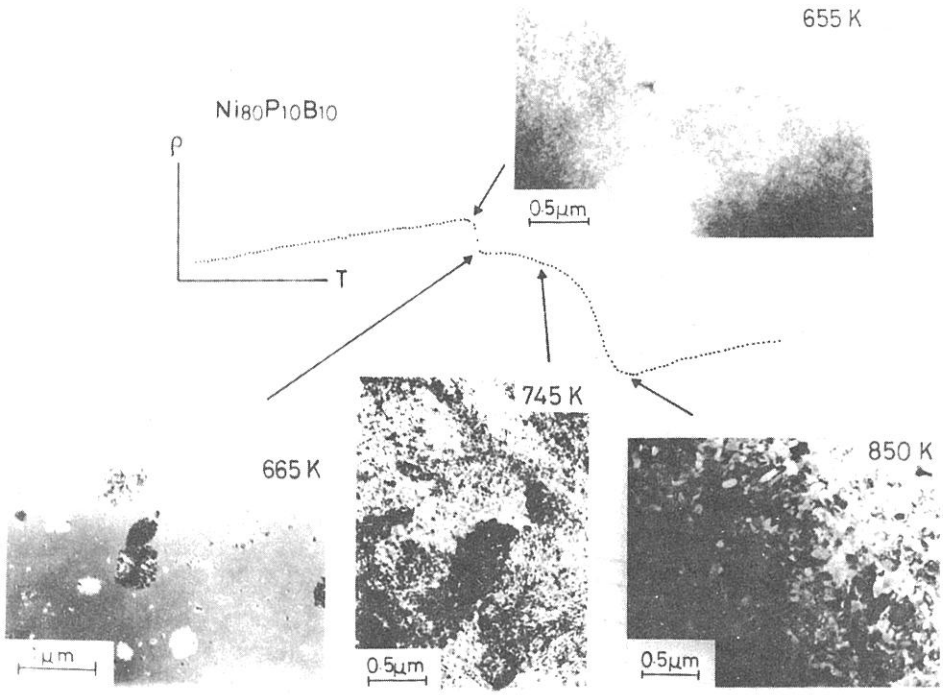

Figure 5. Transmission electron micrographs of amorphous $Ni_{80}P_{10}B_{10}$. Specimens show the microstructure at various stages along the resistivity vs. temperature curve as indicated by arrows.

alloy due to heating to 655 K, 665 K, 745 K and 850 K. At 655 K, small particles (less than 0.1 μm in diameter) could be seen in the amorphous matrix. At 665 K, there appeared a metastable phase with diameters less than 1 μm again in the amorphous matrix. At 745 K, the specimen was entirely transformed to the metastable structure and no amorphous phase remined. At 850 K, recrystallization occurred almost all over the specimen. The size of the recrystallized grains were about the same each other.

Fig. 6 shows the structural changes in the $Ni_{80}P_{15}B_5$ amorphous alloy after heating to 630 K, 660 K and 730 K. At 630 K, the matrix was amorphous and small particles (about 0.5 μm in diameter) could be seen. At 660 K, the specimen was covered almost entirely by metastable phase. At 730 K, recrystallization was virtually complete. The lattice fringes were seen in one of the recrystallized grains.

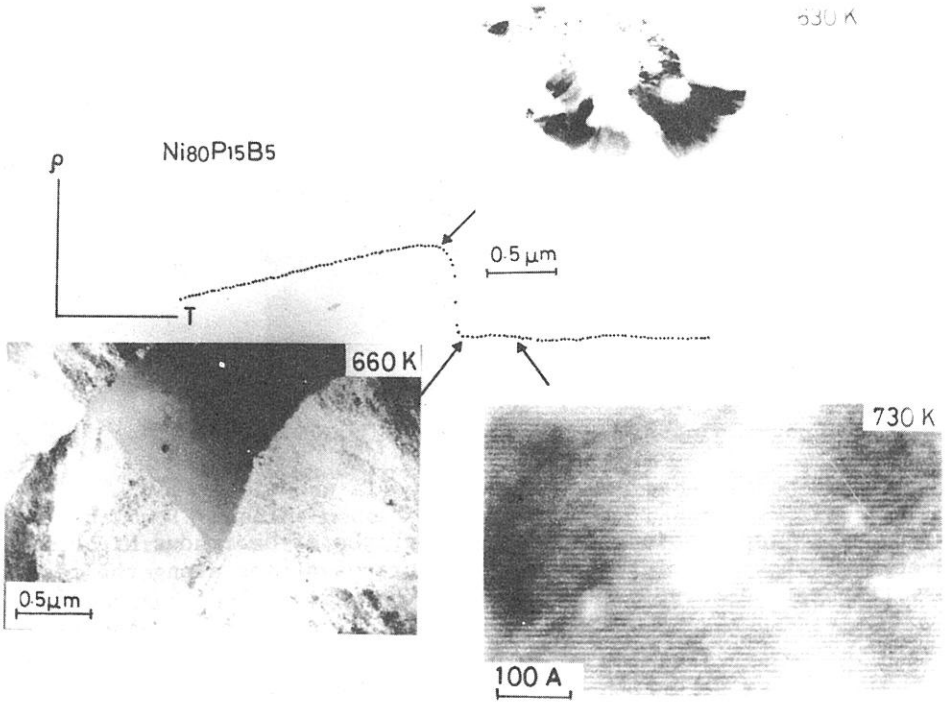

Figure 6. Transmission electron micrographs of amorphous $Ni_{80}P_{15}B_5$. Specimens show the microstructure at various stages along the resistivity vs. temperature curve as indicated by the arrows.

Fig. 7 shows the structural changes after heating to 615 K, 650 K, 740 K and 980 K in $Ni_{80}P_5B_{15}$ amorphous alloy. At 615 K, small metastable particles (about 0.4 ~ 0.2 μm in diameter) could be seen in the amorphous matrix. At 650 K, the specimen was covered almost with metastable phase. At 740 K, particles nearly same size were seen and fringes were deserved at the interface of each particle. At 980 K, the fringes in these particles had disappeared and dislocations could be seen in some of these particles: the crystallization was thought to be complete at this stage.

Fig. 8 shows the temperature in which the resistivity changes with heating from room temperature to 1000 K for each specimen of the $Ni_{80}(P_xB_{1-x})_{20}$ system. From this graph the temperature in which electrical resistivity begins to decrease is the highest in the $Ni_{80}P_{10}B_{10}$ amorphous alloy, so that it can be concluded that this alloy attains the highest thermal stability in these alloys. Also, the temperature range over which the resistivity changes after crystallization is nearly proportional to the content of boron.

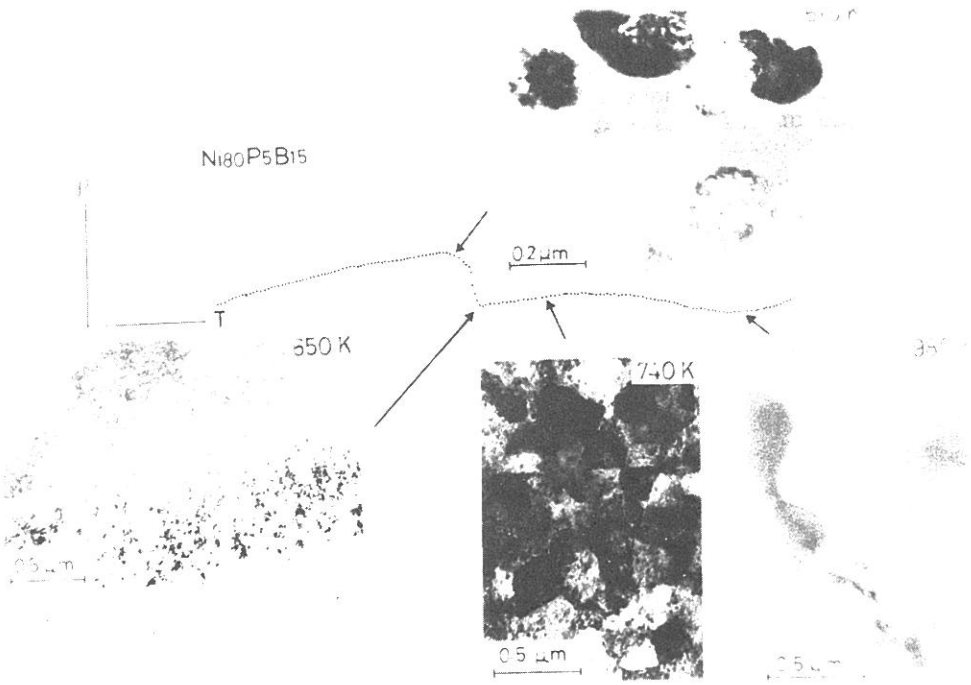

Figure 7. Transmission electron micrographs of amorphous $Ni_{80}P_5B_{15}$. Specimens show the microstructure at various stages along the resistivity vs. temperature curve as indicated by the arrows.

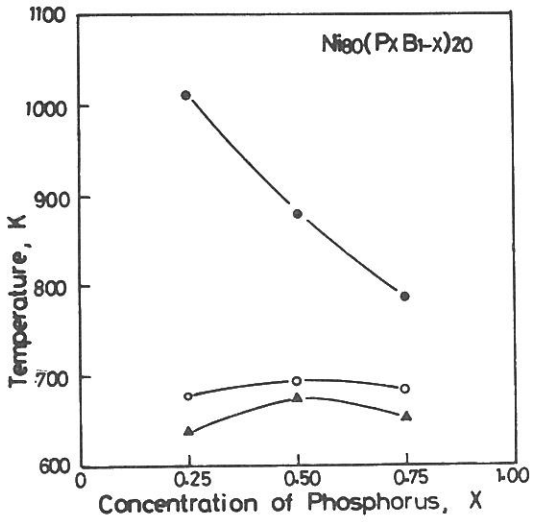

Figure 8. Critical temperature of transformation vs. content of P in the $Ni_{80}(P_xB_{1-x})_{20}$ amorphous alloys.

THE DECREASE IN ELECTRICAL RESISTIVITY DUE TO DEFORMATION

Fig. 9 illustrates the room-temperature tensile properties of liquid-

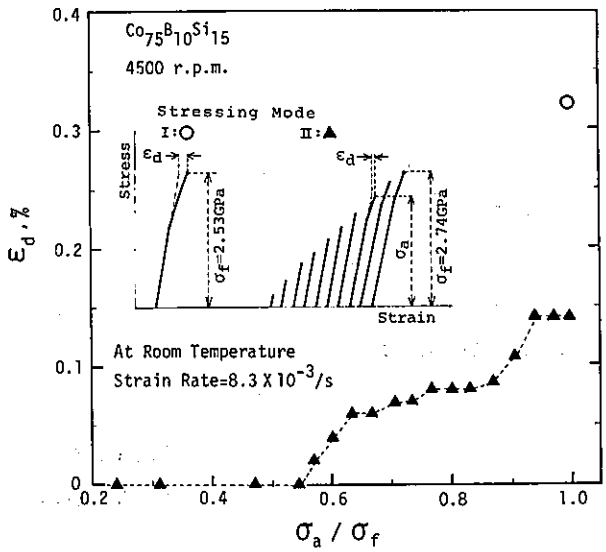

Figure 9. Mechanical properties of liquid-quenched Co-B-Si amorphous alloy. σ_a: maximum applied stress at each stressing cycle, ε_a: deviation from linearity at σ_a of each stressing cycle, σ_f: fracture strength.

quenched $Co_{75}B_{10}Si_{15}$ amorphous alloy. When the amorphous ribbon was deformed in tension (stressing mode I as indicated in the figure) the stress-strain curve was not straight and a deviation from linearity was observed at fracture. However, after a stress of load-unload stressing cycles in which the maximum tensile stress of each cycle was gradually increased (stressing mode II), each stress-strain curve became straighter and the deviation from linearity at fracture was markedly decreased. Furthermore, when the amorphous ribbon which had already been subjected to load- unload stressing cycles at constant tensile stress amplitude was deformed in tension, the deviation from linearity at fracture was markedly decreased. For example, when the Co-B-Si amorphous ribbon was deformed in tension after a tensile stress of 0.98 GPa (the ratio of the maximum applied stress (σ_a) to the fracture strength (σ_f) was about 0.4) had been applied for 200 cycles, the deviation from linearity at fracture was decreased to 0.14 percent, namely, less than half the value obtained for the aforementioned simple tensile deformation (stressing mode I). While in the case of Co-B-Si amorphous ribbon, which was deformed in tension up to various stress levels (i.e., σ_a / σ_f= 0.2 - 0.9) in advance and then fractured in tension (i.e., fractured at the second stressing cycle), no remarkable change in the deviation from linearity at fracture was observed as compared with the case of the stressing mode I. Hence, it is concluded that a cyclic deformation causes a decrease in the deviation from linearity at fracture.

Scanning electron microscope (SEM) observations of the ribbon, which had been deformed and fractured in stressing mode I, revealed the occurrence of many shear deformation bands. However, in the case of the ribbon which had been deformed and fractured in the stressing mode II, shear deformation bands could not be detected by SEM observations. In addition, it was found that cyclic deformation tended to increase the fracture strength (σ_f).

Fig. 10 shows the variation in electrical resistivity as a function of annealing temperature. The curves were obtained (a) from ribbon in the

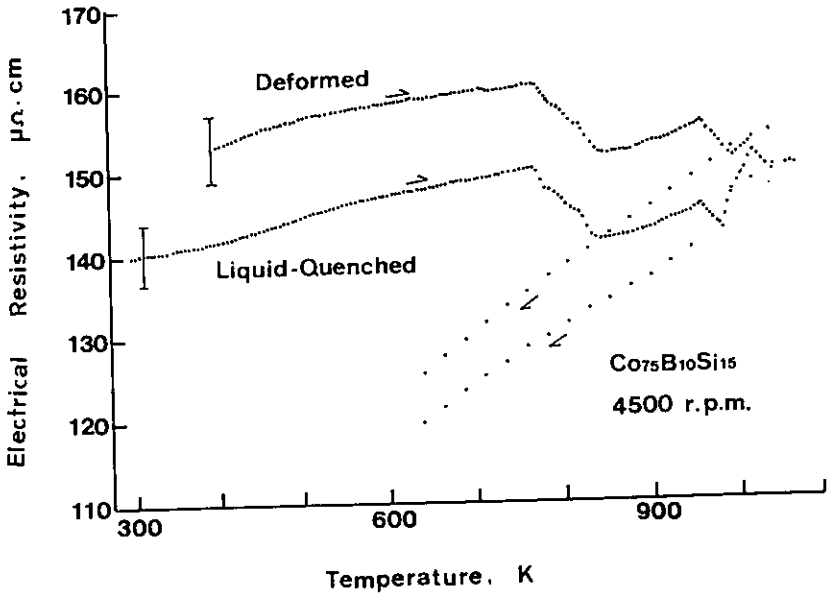

Figure 10. Effect of feformation on the temperature dependence of electrical resistivity of a liquid-quenched Co-B-Si amorphous alloy.

liquid-state and (b) from ribbon which had been deformed and fractured in stressing mode II. From this figure, it is concluded that deformation increases the electrical resistivity of liquid-quenched amorphous alloy. The increase in resistivity, the change in stress-strain behavior and the suppression of the formation of shear deformation bands suggest that the cyclic deformation caused some rearrangements of atoms in the liquid-quenched amorphous alloy. Megusar, Vander Sande and Grant[11] suggested the possibility that phase transformation may occur in amorphous alloy during fatigue deformation. In the present experiments, it is not clear whether the rearrangement of atoms tends to increase or decrease the crystallinity (i.e., to increase the "randomness") in the amorphous structure.

CONCLUSION

According to the results it can be concluded that so-called amorphous alloys do not have one definite atomic arrangement but have a variety of arrangements depending on the quenching rate, the ratio of the contents of component metalloids and the amount of deformation after quenching, etc.

REFERENCES

[1] H. Jones: Rep. Prog. Phys. 36 (1973) 1425.
[2] S. Takayama: J. Mater. Sci. 11 (1976) 164.
[3] M. Doi, H. Kosaki, M. Nonoyama, S. Arai and T. Imura: Proc. 5th Int. Conf. High Voltage Electron Microscopy, Kyoto, 1977, J. Electron Microsc. 26 (1977) Suppl. p. 471.
[4] T. Imura, M. Doi and H. Kosaki: Sci. Rep. RITU, A (1978) June, Suppl. p. 47.
[5] M. Doi, H. Kosaki and T. Imura: Rapidly Quenched Metals III, ed. B. Cantor (The Metals Society, London, 1978) Vol. 2, p. 372.
[6] A. Berrada, M.F. Lapierre, B. Logel, P. Panissod and C. Lobert: Phys. F: Metal. Phys. 8 (1978) 845.
[7] P.J. Cote: Solid State Commun. 18 (1976) 1311.
[8] R.W. Cochrane, R. Harris, J.O. Ström-Olsen and M.J. Zuckermann: Phys. Rev. Lett. 35 (1975) 676.
[9] R. Hasegawa and C.C. Tsuei: Phys. Rev. B 3 (1971) 214.
[10] S.C.H. Lin: J. appl. Phys. 40 (1969) 2173.
[11] J. Megusar, J.B. Vander Sande and N.J. Grant: Rapidly Quenched Metals, ed. N.J. Grant and B.C. Giessen (MIT, Boston, 1976) p. 401.